Mask induced polarization

Andrew Estroff, Yongfa Fan, Anatoly Bourov, Frank Cropanese,
Neal Lafferty, Lena Zavyalova, Bruce Smith
Rochester Institute of Technology, Microelectronic Engineering,
Rochester, NY 14623

ABSTRACT

The objective of this paper is to study the polarization induced by mask structures. Rigorous coupled-wave analysis (RCWA) was used to study the interaction of electromagnetic waves with mask features. RCWA allows the dependence of polarization effects of various wavelengths of radiation on grating pitch, profile, material, and thickness to be studied. The results show that for the five different mask materials examined, the material properties, mask pitch, and illumination all have a large influence on how the photomask polarizes radiation.

Keywords: Photomask, Polarization, Immersion Lithography, High NA, Wire-Grid Polarizer

1. INTRODUCTION

As smaller device dimensions are explored with ever increasing numerical apertures, polarization effects at the mask plane become a concern. For a targeted half pitch resolution of hp, where:

$$hp = \frac{0.5\,l}{(s\ +1)\cdot NA}, \tag{1}$$

the pitch values (Λ) on a photomask are driven to dimensions multiplied by the optical system reduction as:

$$\Lambda_{mask} = \frac{l \cdot M}{(s\ +1)\cdot NA} \tag{2}$$

Assuming $M = 4$, $NA = 0.85$, and σ = 1.0 for current generation tools, $\Lambda_{mask} = 2.35 \cdot l$. Next generation tools moving towards $NA = 1.2$ will result in a minimum mask period of $1.67 \cdot l$, at which point there can be more significant polarization effects contributed by the photomask. The purpose of this paper is to examine these polarization effects induced by the mask features at various numerical apertures, wavelengths, mask pitches, and for different materials.

2. HIGH NA IMAGING AND POLARIZATION

2.1 High NA

TE polarization is defined as polarization perpendicular to the plane of incidence. Radiation polarized in the plane of incidence is referred to as TM polarized. This is shown in Figure 1. As NA increases, the angle of incidence at the wafer's surface becomes more oblique. For TE polarization, there is no decrease in image contrast due to increased angle of incidence. For TM polarization, as the angle of incidence approaches forty-five degrees, the image contrast decreases until it reaches zero at forty-five degrees. This clearly highlights the importance of incorporating polarization into lithography modeling and simulation. Smith and Cashmore have demonstrated the invalidity of a previously useful metric (aerial image evaluation) in systems incorporating high NA and polarization[1].

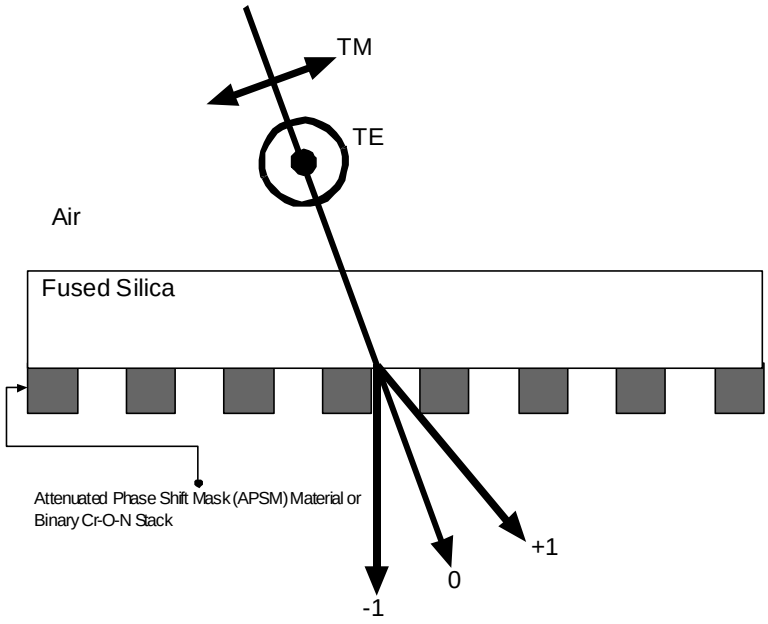

Figure 1. Unpolarized light incident upon photomask

2.2 Wire Grid Polarization

Wire-grid polarizers function according to the following basic principles. The electric field of the TE polarized light induces a current in the wires. The forward transmitted radiation is out of phase with the incident TE wave and thus has greatly reduced intensity, and the backward transmitted radiation is measured as the reflected wave. The electric field of the TM polarized light is perpendicular to the wires. The wires are very narrow in this dimension and the electrons have very little room to move. Therefore, most of the TM radiation is transmitted unaffected[2]. This is shown in Figure 2.

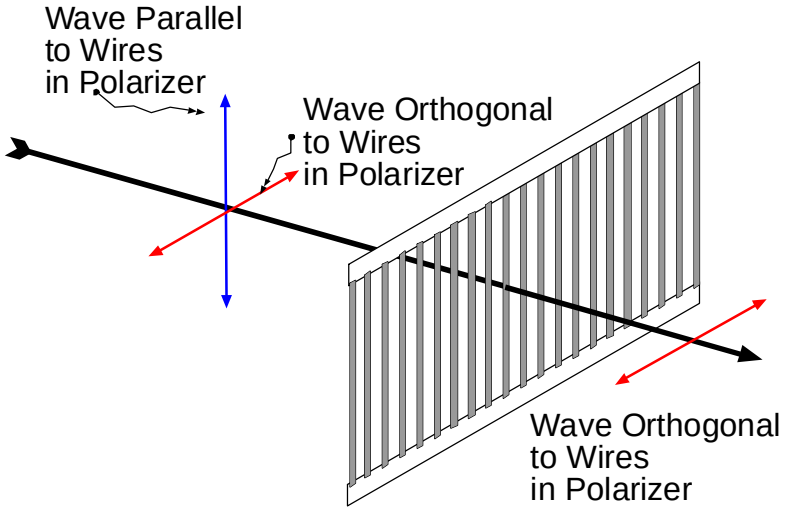

Figure 2. Wire-Grid Polarization

The parameters which impact the efficiency of a wire-grid polarizer include period, duty cycle, thickness, shape, and material. The grating period is the most important of these parameters as it determines the minimum wavelength that can be polarized for a specific diffracted order, as shown in Equation 3. As the period decreases, wires become closer together making it easier for TE polarization to induce a current in the wires. Additionally, narrower wires attenuate the TM mode less, thus passing TM polarization more efficiently. Duty cycle is defined as the wire width divided by the period. Assuming a fixed period, if the duty cycle increases, so does the wire width, attenuating both the TE and TM polarizations more. Again, as in the case for decreasing period, a larger duty cycle will result in a more efficient TM polarizer. As grating thickness increases, the wires are able to generate more current, creating a more efficient polarizer. The shape of the wires also has an effect on the transmission and polarization efficiency. Non-vertical sidewalls cause a decrease in transmission, but do not have much effect on the polarization efficiency. Rounded edges will slightly reduce transmission, however, with greater rounding, there is a greater loss in transmission. Rounded edges will also shift the peak transmission to shorter wavelengths. Most importantly, rounded edges will result in a decrease in polarization efficiency, a benefit to the lithographer.

Wood first noticed a sharp decrease in transmission in the transition region of wire-grid polarizers in 1902.[3] This phenomenon became known as Wood's Anomalies. In 1907, Lord Rayleigh analyzed Wood's data and noted that for a specific wavelength (l), period (Λ), material refractive index (n), and angle of incidence (q), a higher diffracted order (m) emerges, as [4]:

$$l = \frac{\Lambda \cdot (n \pm \sin q)}{m} \tag{3}$$

Another phenomenon that occurs in the transition region for wire-grid polarizers is the transmission of TE polarization as opposed to TM polarization in Chromium gratings. These have been studied by Honkanen et al, and are appropriately named inverse polarizers [5].

2.3 Mask induced polarization

Asymmetry is what gives rise to polarization due to the different behaviors of orthogonally polarized incident waves. In photomasks the asymmetry is contributed to by the dimensions of the features. These features can not be sufficiently approximated by assuming that they are a grating comprised of a thin metal film on a dielectric substrate. For feature sizes greater than twice the wavelength, a diffraction grating results with little to no polarization effects. For feature sizes less than half of the wavelength, the mask acts as a zero order wire-grid polarizer. Between half and twice the wavelength is a transition region where the mask polarizes and diffracts the radiation, and can act as an inverse polarizer for some materials.

3. EXPERIMENTAL SETUP

This purpose of this experiment is to demonstrate the polarization effects induced by a photomask. A binary $Cr_xO_yN_z$-on-glass mask was modeled using an effective media approximation using data from materials deposited via magnetron sputtering and characterized using ultra-violet variable angle spectroscopy (UV-VASE) [6]. The four layer stack described in Tables 1 and 2 represent the graded $Cr_xO_yN_z$ stack.

	Layer 1	**Layer 2**	**Layer 3**	**Layer 4**
Cr	90.00%	18.90%	9.45%	0.00%
CrN	10.00%	2.10%	1.05%	0.00%
CrOx	0.00%	79.00%	89.50%	100.00%

Table 1. Cr-O-N stack composition. Layer 1 is closest to substrate, layer 4 is furthest.

	Layer 1		Layer 2		Layer 3		Layer 4	
	193nm	**248nm**	**193nm**	**248nm**	**193nm**	**248nm**	**193nm**	**248nm**
n	0.8209	0.8863	1.5649	1.8142	1.6740	1.9734	1.7782	2.1260
k	1.1825	1.8700	0.4121	0.7391	0.3597	0.6584	0.3148	0.5918
Thickness (A)	500	500	133	133	133	133	133	133

Table 2. Cr-O-N stack data. Layer 1 is closest to substrate, Layer 4 is furthest.

Attenuated Phase Shifting Mask (APSM) materials were also modeled. APSM materials chosen were Tantalum Nitride in a Silicon Nitride host (TaN-Si_3N_4), Molybdenum Oxide in a Silicon Dioxide host (MoO_3-SiO_2), Silicon in a Silicon Nitride host (Si-Si_3N_4), and Tantalum Oxide in a Silicon Dioxide host (TaO_5-SiO_2). These materials were also modeled using the effective media approximation described earlier. All masking films were designed for a π phase shift and 10% transmission. Tables 3 and 4 contain the APSM material data.

	TaN-Si3N4		Si-Si3N4		MoO3-SiO2		Ta2O5-SiO2	
	TaN	***Si3N4***	Si	***Si3N4***	MoO3	***SiO2***	Ta2O5	***SiO2***
157nm	X	X	X	X	10.0%	90.0%	11.5%	88.5%
193nm	17.0%	83.0%	9.0%	91.0%	30.0%	70.0%	X	X
248nm	27.0%	73.0%	10.0%	90.0%	27.0%	73.0%	X	X

Table 3. APSM material composition. Host material in bold and italics.

	TaN-Si3N4		Si-Si3N4		MoO3-SiO2			Ta2O5-SiO2
	193nm	**248nm**	**193nm**	**248nm**	**157nm**	**193nm**	**248nm**	**157nm**
n	2.5626	2.3833	2.4317	2.3482	1.6253	1.5891	1.6458	1.704
k	0.489	0.433	0.4462	0.4246	0.223	0.2117	0.2246	0.2468
Thickness (A)	631	913	687	936	1262	1647	1932	1122
% Transmission	9.88	10.37	10.4	10.35	9.8	9.69	10.28	10.02

Table 4. APSM material data.

Rigorous Coupled Wave Analysis (RCWA) provides an exact solution for Maxwell's equations [7]. Several commercially available grating simulation software packages have emerged using RCWA. GSOLVER was used to perform this experiment [8]. GSOLVER is a visual grating structure editor utilizing full 3-dimensional vector code using hybrid RCWA and modal analysis and is capable of analyzing arbitrary grating thickness, number of materials, and material index of refraction. Additionally, it is capable of modeling multiple materials, buried structures, and varied shapes (represented by stacked layers).

Unpolarized radiation was modeled by first inputting a 100% TE polarized beam and measuring the transmitted TE intensity in the 0^{th} and 1^{st} diffracted orders and then inputting a 100% TM polarized beam and measuring the transmitted TM intensity in the 0^{th} and 1^{st} diffracted orders. This was done for 157nm, 193nm, and 248nm radiation depending on the mask material. The mask pitch was varied from 0nm to 1000nm (1um) in 10nm increments, while the duty cycle was kept fixed at 0.5. Degree of Polarization (shown in equation 4 below) was plotted versus mask pitch for the different materials and wavelengths.

$$DoP = \frac{T_{TE} - T_{TM}}{T_{TE} + T_{TM}} \tag{4}$$

A degree of polarization of –1 signifies fully TM polarized radiation, +1 signifies fully TE polarization, and 0 means equal TE and TM polarization.

The masks were modeled at all of the wavelengths listed for the specific material in Tables 2 and 4. All masks were modeled with the light incident at 0 degrees, except for the binary mask, which was also modeled for an off axis illumination of NA = 1.2 and magnification of 4x which corresponds to 16.9 degrees in air, 11.5 degrees in quartz.

4. RESULTS

If the Wood's Anomaly equation is rearranged into equation 5, the grating pitch at which a particular order emerges is given.

$$\Lambda = \frac{m \cdot l}{n \pm \sin q} \tag{5}$$

For all on axis cases in this experiment, this corresponds to the first order emerging at $\Lambda = l$. For all APSM material cases, the 0^{th} order (Figures 3,5,7,9,11,13,15,17,19) experiences a sharp decrease in transmission at $\Lambda = l$. The on-axis illumination of the binary mask also has its first orders emerging at a mask pitch equal to l however it does not experience the same sharp drop in transmission.

Overall, for materials with similar n and k values, the transmission and degree of polarization (DoP) results are quite similar. To prevent great repetition in the analysis, TaO_5-SiO_2 and MoO_3-SiO_2 will be considered together for the 157nm illumination case, and TaN-Si_3N_4 and Si-Si_3N_4 for the 193 and 248nm cases.

The APSM materials act as relatively efficient polarizers when illuminated with 157nm radiation (Figures 3-6). Below $\Lambda=\lambda$, they have the highest 0^{th} order transmission. At a Λ very near λ, they are very efficient polarizers, passing 100% TM polarized radiation. However, this is also where the +/-1^{st} orders emerge and transmission drops to a minimum, below 5%. As mask pitch increases, so does transmission, while the TM polarization efficiency decreases. The DoP for the +/-1^{st} orders remains near 0 except in the region where $\lambda<\Lambda<2\lambda$, where more TM polarization is passed. At $\Lambda = 2\lambda$, the mask passes equal TE and TM polarized radiation.

For 193nm radiation (Figures 7-12), the APSM materials' transmission follows the same trends that the 0^{th} and 1^{st} orders followed in the 157nm case. The 0 order is transmitted most below $\Lambda=\lambda$, is a minimum at approximately $\Lambda=\lambda$, and increases slowly to 10% as Λ increases. The 1^{st} orders emerge at $\Lambda=\lambda$, and the transmission slowly increases until $\Lambda=2\lambda$ where it levels off at about 17%. For TaN-Si_3N_4 (Figure 7) and Si-Si_3N_4 (Figure 9) the 0^{th} order is polarized predominantly TM, with maximum efficiency of DoP close to –1 just above and below $\Lambda=\lambda$. At $\Lambda=\lambda$, there is a sharp decrease in polarization efficiency. The 1^{st} orders (Figures 8 and 10) are polarized predominantly TM (maximum DoP near –0.5) at $\Lambda=\lambda$, and essentially decrease in efficiency linearly with mask pitch until $\Lambda=2\lambda$, where they are polarized equally 50% TE and 50% TM. For the MoO_3-SiO_2 case, the 0^{th} order (Figure 11) is polarized predominantly TM, however, just below $\Lambda=\lambda$ there is a sharp decrease in efficiency towards DoP=0, followed by a sharp increase in efficiency until DoP=-1 at a Λ slightly greater than λ. Polarization efficiency steadily decreases as Λ becomes greater. The 1^{st} orders (Figure 12) are polarized slightly more TM (between DoP of 0 and –0.2) at $\Lambda=\lambda$ and remain so until $\Lambda=2\lambda$ where the polarization efficiency decreases back to DoP=0. For the 248nm illumination of the APSM materials (Figures 13-18), all results follow the same trends from the 193nm case with a few slight differences in the extrema.

In the case of the 193nm on-axis illumination of the binary $Cr_xO_yN_z$ mask (Figures 19 and 20), the 0^{th} order transmission decreases to a minimum of just under 15% as Λ approaches λ., then increases sharply to just above 20% at $\Lambda=\lambda$, after which it continuously increases to slightly over 25% at Λ=1000nm. The 0^{th} order DoP is approximately –0.5 (75% TM, 25% TE) until $\Lambda=\lambda$, at which it rapidly loses efficiency and briefly acts as an inverse polarizer, and then remains close to 0 from just past $\Lambda=\lambda$ to Λ=1000nm. The +/-1^{st} orders arise at $\Lambda=\lambda$ and consistently transmit 6-7% until $\Lambda=2\lambda$ where their transmission increases to and remains at about 8%. The +/-1^{st} orders are polarized predominantly TE (DoP ~0.2) at $\Lambda=\lambda$, and slowly loses efficiency as Λ increases.

For 193nm off-axis illumination of the binary $Cr_xO_yN_z$ mask (Figures 23, 25, and 27), the 0^{th} order transmission follows a similar trend to that in the 193nm on-axis case, however it increases sharply at there both the $+1^{st}$ and -1^{st} orders emerge, which is at $\Lambda=3\lambda/4$ and $\Lambda=3\lambda/2$ respectively. After the $+1^{st}$ order begins to propagate, the transmission slowly increases towards 25% as Λ approaches 1000nm. The 0^{th} order is polarized predominantly TM (DoP=-0.5) below the

mask pitch at which the -1^{st} order emerges. At this pitch the 0^{th} order rapidly loses polarization efficiency to a DoP of about –0.2, where it remains relatively constant until the mask pitch approaches the pitch at which the $+1^{st}$ order emerges. At this pitch there is again a rapid decrease in the polarization efficiency, for a brief period the mask acts as a weak inverse polarizer, and then passes equal amounts of TE and TM past a pitch of 400nm. The -1^{st} order transmission is roughly 5% from $\Lambda=3\lambda/4$ until the $+1^{st}$ order emerges at $\Lambda=3\lambda/2$, where it rises sharply and remains relatively constant at approximately 7%. The -1^{st} order is polarized more TE than TM and reaches its maximum polarization efficiency at a DoP=0.4 at $\Lambda=3\lambda/2$ where the $+1^{st}$ order emerges, then loses efficiency and approaches a DoP=0 as pitch increases. The $+1^{st}$ order emerges at $\Lambda=3\lambda/2$ and increases in transmission from 5% to 9% at $\Lambda=3\lambda$, after which it remains steady. It is polarized slightly TM until it's maximum TM polarization efficiency at about $\Lambda=2\lambda$, and becomes slightly more TE polarized as pitch increases until it reaches its maximum TE polarization efficiency with a DoP=0.09 near $\Lambda=3\lambda$, after which DoP decreases back towards 0 as pitch increases.

Besides some subtle differences, the 248nm on-axis illumination of the binary $Cr_xO_yN_z$ mask (Figures 21 and 22) generates very similar trends to the 193nm on-axis case for transmission and polarization efficiency. One notable difference is that the 0^{th} order has greater extrema. The 0^{th} order transmission begins higher at a value near 30%, then sharply drops to near 10% at Λ=150nm, and then increases with mask pitch to near 25% transmission at Λ=1000nm. The 0^{th} order has a DoP of about –0.9 at the minimum pitch and loses efficiency until $\Lambda=\lambda$ where it briefly acts as a weak inverse polarizer, and at larger pitches is polarized equally TE and TM. The $+/-1^{st}$ orders emerge at $\Lambda=\lambda$ and follow similar trends as in the 193nm on-axis case. Overall, the transmission of the orders is 1-2% greater than in the 193nm case. The DoP begins slightly more TM, but within a pitch increase of $\lambda/5$, the DoP becomes slightly more TE with a maximum DoP of 0.12 just before $\Lambda=2\lambda$. The mask loses polarization efficiency as pitch increases and slowly moves towards a DoP of 0.

For the 248nm off-axis illumination of the binary $Cr_xO_yN_z$ mask (Figures 24, 26, and 28), very similar patterns to the 193nm off-axis illumination case are observed. The -1^{st} and $+1^{st}$ orders emerge at $\Lambda=3\lambda/4$ and $\Lambda=3\lambda/2$. The 0^{th} order transmission is very similar to the 248nm on-axis case, but with sharp increases as the $+/-1^{st}$ orders emerge, as in the 193nm off-axis case, but with a less-sharp increase with the emergence of the $+1^{st}$ order. The $+/-1^{st}$ order transmissions are very similar to the 248nm on-axis 1^{st} order transmissions, except the $+1^{st}$ order exhibits slightly greater transmissions (1%). As in the 193nm of-axis case, the -1^{st} order is polarized more TE than TM and reaches its maximum polarization efficiency at a DoP of about 0.2 at near $\Lambda=3\lambda/2$ where the $+1^{st}$ order emerges, then loses efficiency and approaches a DoP=0 as pitch increases. However, the -1^{st} order is polarized more TM where it first emerges, then steadily loses its TM polarization efficiency within a change in pitch of $\lambda/5$ after which it functions as mentioned above. The $+1^{st}$ order's polarization follows the same patterns as in the 193nm off-axis case, but exhibits its maximum TM polarization when it first emerges, steadily loses TM polarization efficiency until $\Lambda=2.5\lambda$ where the DoP=0, then TE polarization slightly increases until it reaches a maximum DoP at $\Lambda=3\lambda$, after which as pitch increases the DoP moves towards 0.

Tables 5 and 6 offer summaries of the degrees of polarization for different illumination schemes for different masks at the NA values mentioned in the introduction. The polarization effects induced by the mask at the higher NA are always greater in magnitude than at the lower NA, except for three cases ($Cr_xO_yN_z$ mask 193nm off-axis illumination $+1^{st}$ order and $Cr_xO_yN_z$ mask 248nm on-axis and off-axis illumination 0^{th} order).

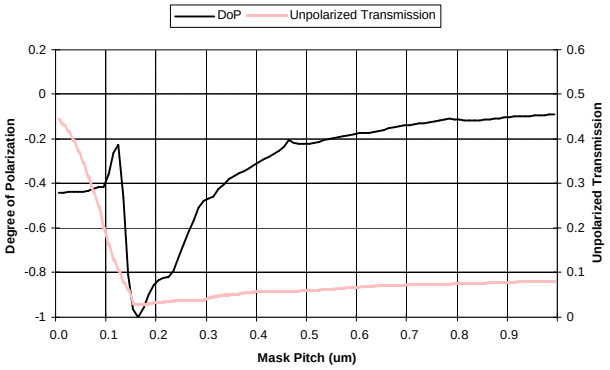

Figure 3. Ta2O5-SiO2 mask, 0th order results for 157nm illumination.

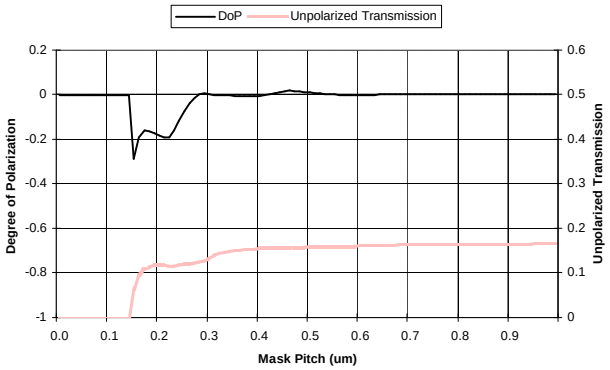

Figure 4. Ta2O5-SiO2 mask, +/- 1st order results for 157nm illumination.

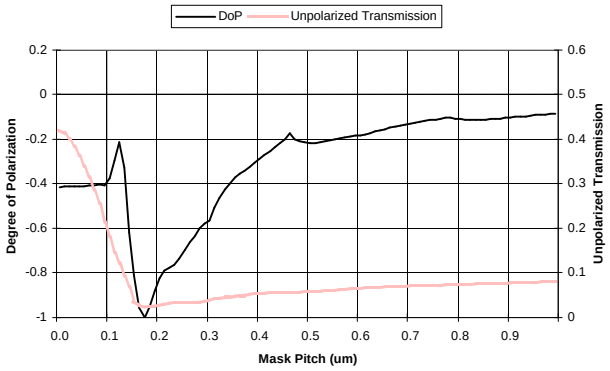

Figure 5. MoO3-SiO2 mask, 0th order results for 157nm illumination.

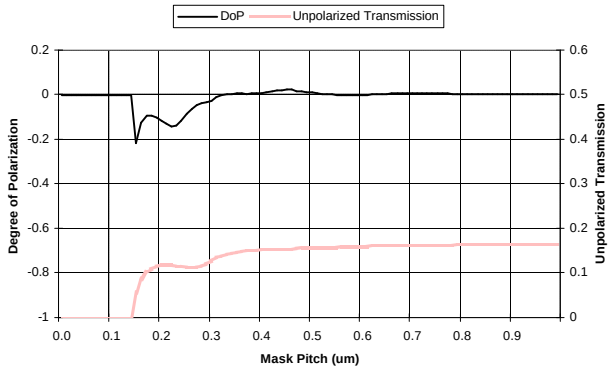

Figure 6. MoO3-SiO2 mask, +/- 1st order results for 157nm illumination.

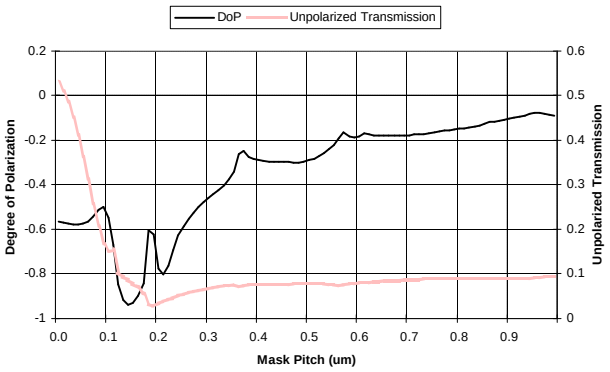

Figure 7. TaN-Si3N4 mask, 0th order results for 193nm illumination.

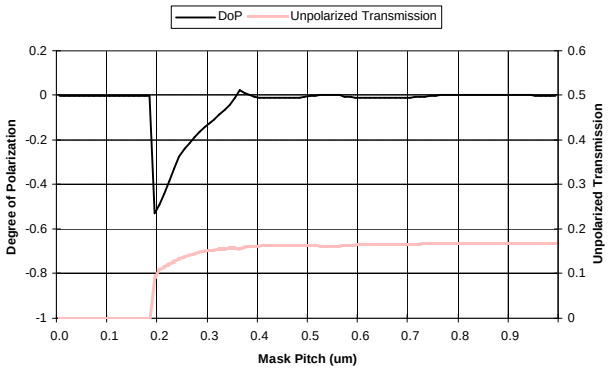

Figure 8. TaN-Si3N4 mask, +/- 1st order results for 193nm illumination.

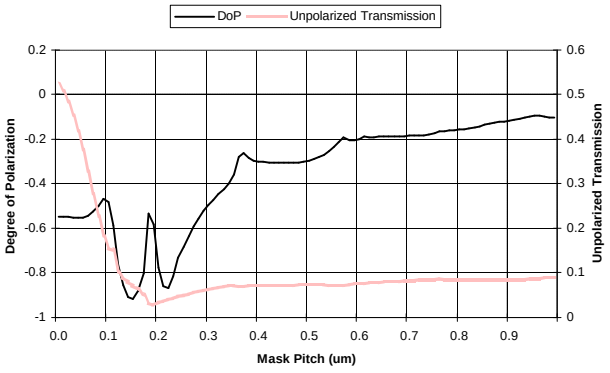

Figure 9. Si-Si3N4 mask, 0th order results for 193nm illumination.

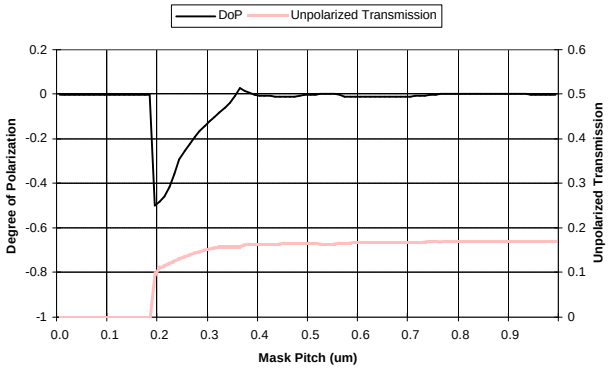

Figure 10. Si-Si3N4 mask, +/- 1st order results for 193nm illumination.

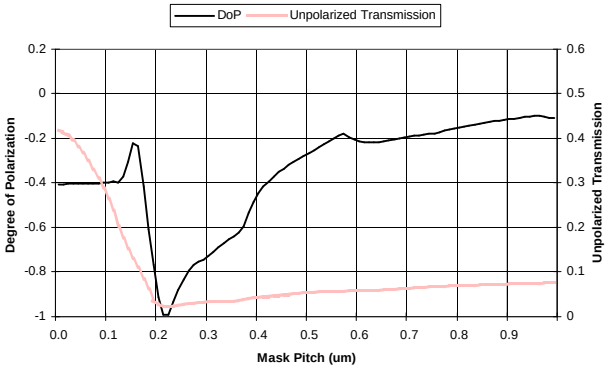

Figure 11. MoO3-SiO2 mask, 0th order results for 193nm illumination.

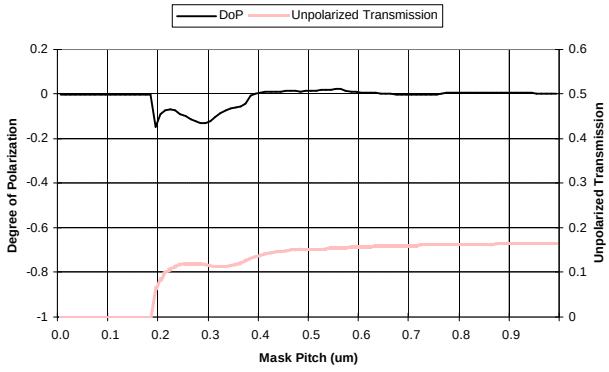

Figure 12. MoO3-SiO2 mask, +/- 1st order results for 193nm illumination.

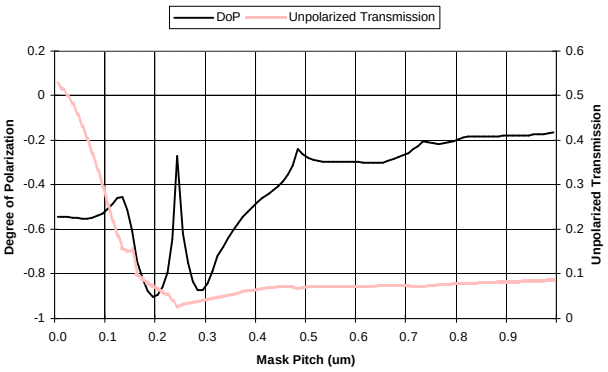

Figure 13. TaN-Si3N4 mask, 0th order results for 248nm illumination.

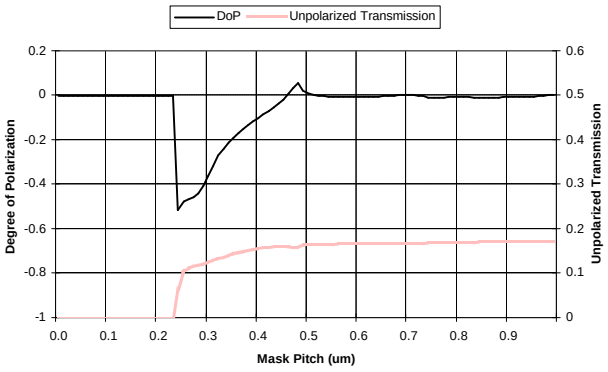

Figure 14. TaN-Si3N4 mask, +/- 1st order results for 248nm illumination.

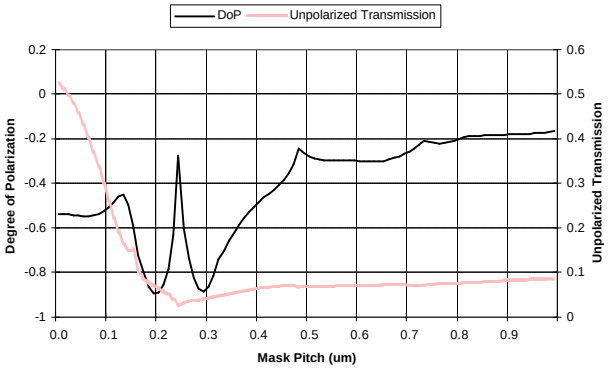

Figure 15. Si-Si3N4 mask, 0th order results for 248nm illumination.

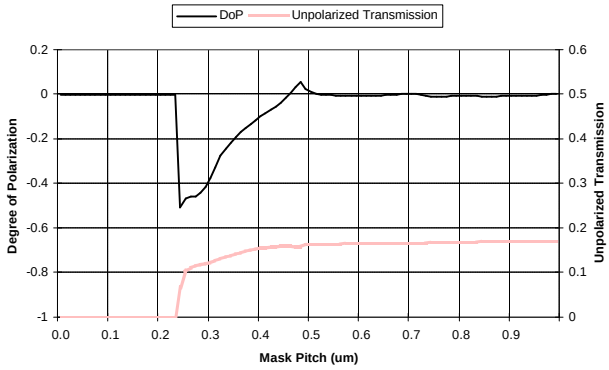

Figure 16. Si-Si3N4 mask, +/- 1st order results for 248nm illumination.

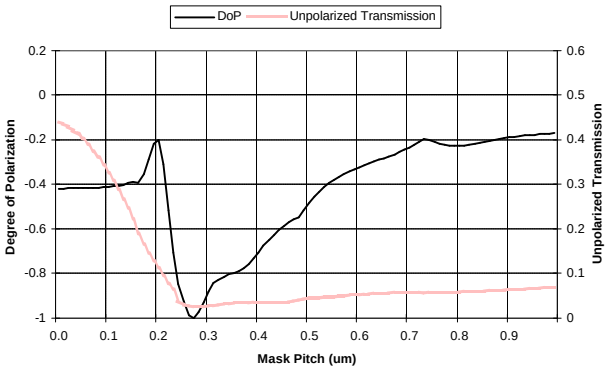

Figure 17. MoO3-SiO2 mask, 0th order results for 248nm illumination.

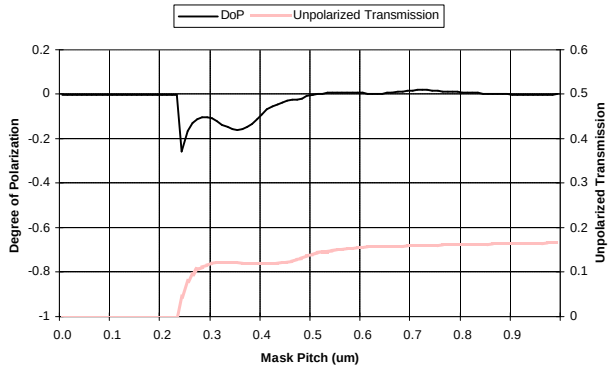

Figure 18. MoO3-SiO2 mask, +/- 1st order results for 248nm illumination.

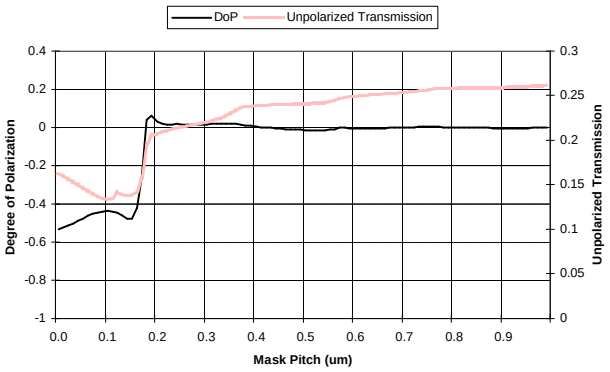

Figure 19. Binary Cr-O-N mask, 0th order results for 193nm illumination.

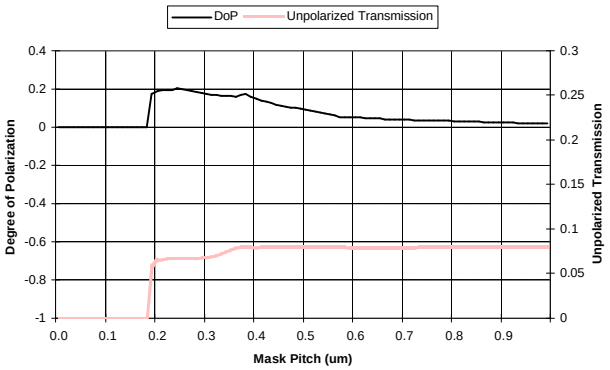

Figure 20. Binary Cr-O-N mask, +/- 1st order results for 193nm illumination.

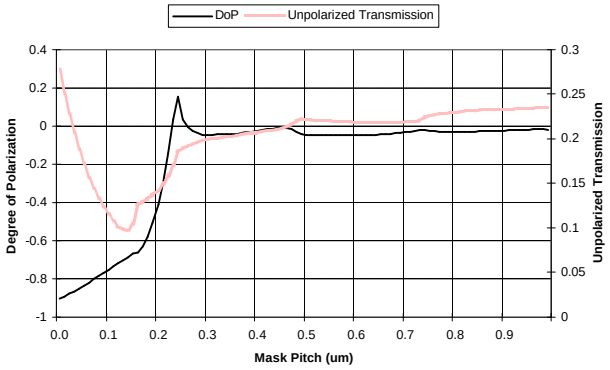

Figure 21. Binary Cr-O-N mask, 0th order results for 248nm illumination.

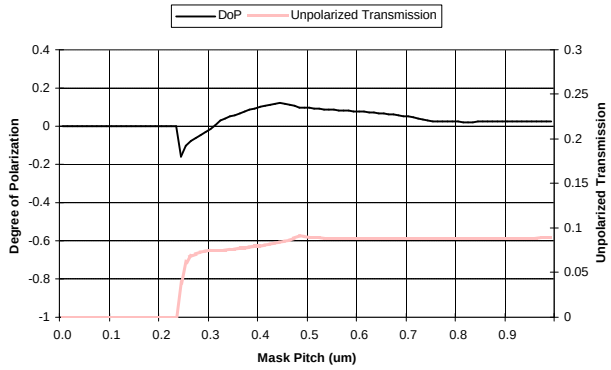

Figure 22. Binary Cr-O-N mask, +/- 1st order results for 248nm illumination.

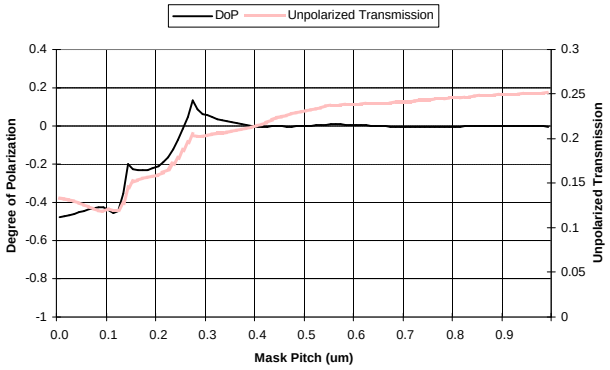

Figure 23. Binary Cr-O-N mask, 0th order results for 193nm off-axis illumination.

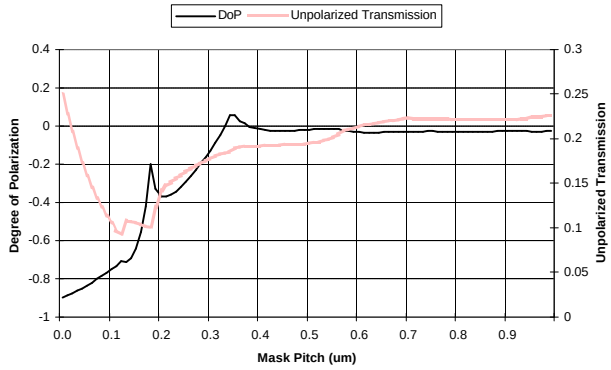

Figure 24. Binary Cr-O-N mask, 0th order results for 248nm off-axis illumination.

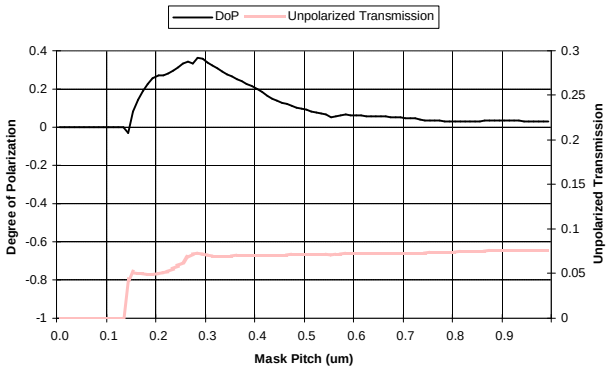

Figure 25. Binary Cr-O-N mask, -1st order results for 193nm off-axis illumination.

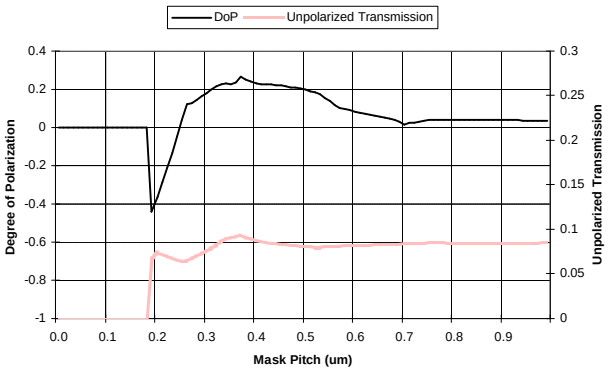

Figure 26. Binary Cr-O-N mask, -1st order results for 248nm off-axis illumination.

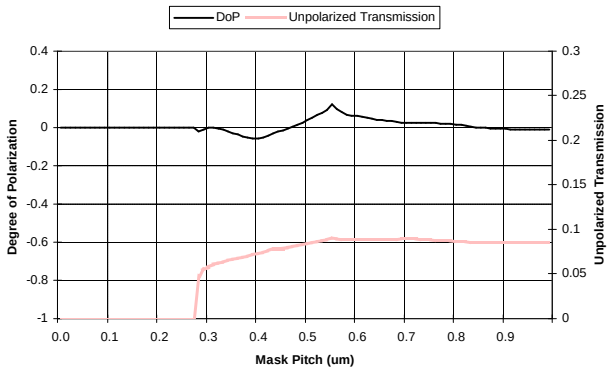

Figure 27. Binary Cr-O-N mask, +1st order results for 193nm off-axis illumination.

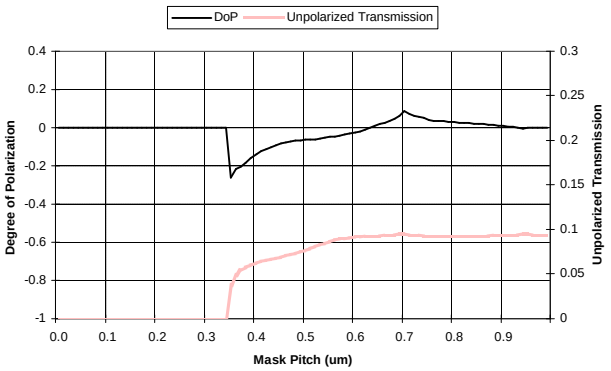

Figure 28. Binary Cr-O-N mask, +1st order results for 248nm off-axis illumination.

Wavelength	157nm				193nm				248nm			
Order	0th		1st		0th		1st		0th		1st	
NA	0.85	1.2	0.85	1.2	0.85	1.2	0.85	1.2	0.85	1.2	0.85	1.2
Ta2O5	-0.353	-0.671	-0.006	-0.07	x	x	x	x	x	x	x	x
TaN	x	x	x	x	-0.297	-0.442	-0.013	-0.107	-0.298	-0.476	-0.008	-0.102
Si	x	x	x	x	-0.304	-0.471	-0.009	-0.102	-0.299	-0.484	-0.007	-0.1
MoO3	-0.354	-0.698	0.004	-0.087	-0.351	-0.709	0.013	-0.102	-0.353	-0.703	0.006	-0.089

Table 5. Degree of polarization values for particular NA for APSM materials.

Wavelength	193nm						248nm					
Order	0th		-1st		+1st		0th		-1st		+1st	
NA	0.85	1.2	0.85	1.2	0.85	1.2	0.85	1.2	0.85	1.2	0.85	1.2
Cr-O-N	-0.004	0.018	0.12	0.171	0.12	0.171	-0.049	-0.026	0.082	0.102	0.082	0.102
Cr-O-N OAI	-0.001	0.045	0.137	0.323	-0.021	0	-0.025	-0.016	0.104	0.231	-0.042	-0.136

Table 6. Degree of polarization for particular NA for binary Cr-O-N mask.

5. CONCLUSION

Rigorous Coupled Wave Analysis was used to solve Maxwell's equations for photomasks comprised of alternating phase shift mask materials and for a standard binary $Cr_xO_yN_z$-on-glass. Different materials, radiation wavelength, thickness, pitch, and incident angle all have a great effect on how much a mask will polarize light.

The APSM materials tend to act more like traditional wire-grid polarizers and pass mainly the TM component and for all of the cases a higher NA results in greater polarization. For the binary $Cr_xO_yN_z$-on-glass mask materials, higher NA usually results in a greater polarization contribution from the mask. Additionally, the binary mask material also acts as an inverse polarizer in some circumstances, passing more TE polarization than TM. In the off-axis illumination case, there is significant shadowing of the $+1^{st}$ order from the thickness of the mask material. This is easily seen in figures 25-28 where the $+1^{st}$ order does not begin transmitting until the pitch is significantly larger than in the -1^{st} order case.

Polarization induced by the mask will need to be taken into account. Mask materials that transmit equal amounts of TE and TM polarization are desirable as higher numerical apertures are pursued so that no one polarization state has more weighting than the other, especially the TM state which could have a detrimental impact on image contrast. Concerns regarding polarization mask effects may lead to requirements to increase the reduction factor of projection imaging tools. As 4x reduction may be a concern for sub-45nm generations, 6x or 8x can reduce critical issues.

REFERENCES

1. B. Smith, J. Cashmore, *Challenges in High NA, Polarization, and Photoresists*.
2. J. H. Johnson, *Wire Grid Polarizers for Visible Wavelengths*, PhD dissertation, University of Rochester, Rochester, NY, 2003
3. R. W. Wood, *Uneven Distribution of Light in a Diffraction Grating Spectrum*, Philosophical Magazine, September, 1902
4. Lord Rayleigh, *On the Remarkable Case of Diffraction Spectra Described by Prof. Wood*, Philosophical Magazine, July, 1907
5. Honkanen et al, *Inverse Metal-Stripe Polarizers*, Applied Physics B **68**, 81-85, 1999
6. http://www.rit.edu/~635dept5/
7. M. G. Moharam, T. K. Gaylord, *Rigorous Coupled-Wave Analysis of Planar-Grating Diffraction*, J. Opt. Soc. Am. **71** (7), 811-818, 1981
8. GSOLVER Product Site, http://www.gsolver.com